

# The loss of CO from the *ortho*, *meta* and *para* forms of deprotonated methyl benzoate in the gas phase

2 PERKIN

Andrew M. McAnoy, Suresh Dua, Stephen J. Blanksby and John H. Bowie\*

Department of Chemistry, The University of Adelaide, South Australia, 5005

Received (in Cambridge, UK) 7th April 2000, Accepted 2nd June 2000

Published on the Web 12th July 2000

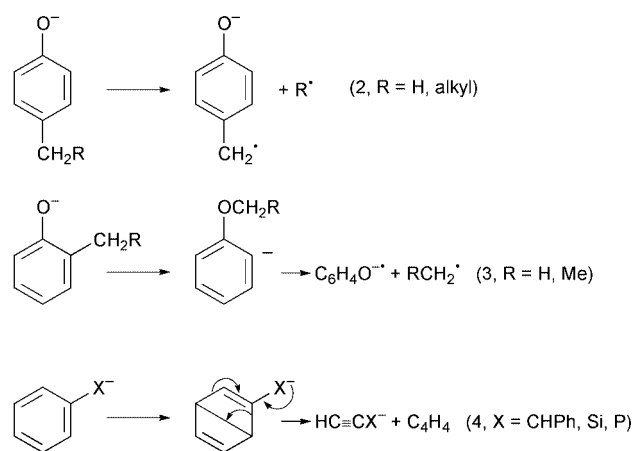
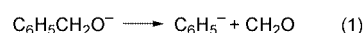
The *ortho*, *meta* and *para* anions of methyl benzoate may be made in the source of a mass spectrometer by the  $S_N2(Si)$  reactions between  $HO^-$  and methyl (*o*-, *m*-, and *p*-trimethylsilyl)benzoate respectively. All three anions lose CO upon collisional activation to form the *ortho* anion of anisole in the ratio *ortho*  $\gg$  *meta*  $>$  *para*. The rearrangement process is charge directed through the *ortho* anion. Theoretical calculations at the B3LYP/6-311++G(d,p)//HF/6-31+G(d) level of theory indicate that the conversion of the *meta* and *para* anions to the *ortho* anion prior to loss of CO involve 1,2-H transfer(s), rather than carbon scrambling of the methoxycarbonylphenyl anion. There are two mechanisms which can account for this rearrangement, *viz.* (A) cyclisation of the *ortho* anion centre to the carbonyl group of the ester to give a cyclic carbonyl system in which the incipient methoxide anion substitutes at one of the two equivalent ring carbons of the three membered ring to yield an intermediate which loses CO to give the *ortho* anion of anisole, and (B) an elimination reaction to give an intermediate benzyne–methoxycarbonyl anion complex in which the  $MeOCO^-$  species acts as a  $MeO^-$  donor, which then adds to benzyne to yield the *ortho* anion of anisole. Calculations at the B3LYP/6-311++G(d,p)//HF/6-31+G(d) level of theory indicate that (i) the barrier in the first step (the rate determining step) of process A is 87 kJ mol $^{-1}$  less than that for the synchronous benzyne process B, and (ii) there are more low frequency vibrations in the transition state for benzyne process B than for the corresponding transition state for process A. Stepwise process A has the lower barrier for the rate determining step, and the lower Arrhenius factor: we cannot differentiate between these two mechanisms on available evidence.

## Introduction

The negative ion spectra of deprotonated neutral organic molecules are generally quite characteristic and diagnostic of structure.<sup>1</sup> In the majority of cases, the spectra are simple, involving either loss of a radical, or a neutral accompanied by a hydrogen transfer reaction. When these cleavage reactions are energetically unfavourable, three scenarios may pertain, *viz.* (i) the initially formed  $(M - H)^-$  ion rearranges (often by H transfer) to another anion which is able to undergo facile cleavage, (ii) the initial anion may undergo a skeletal rearrangement which is often identical to the reaction which occurs for the same system under basic conditions in solution,<sup>2</sup> and (iii) a reaction may take place which occurs remote from and uninfluenced by the anionic centre.<sup>3,4</sup>

Deprotonated phenyl systems containing substituents illustrate a number of these fragmentation types. For example, the benzyloxide anion fragments by the simple cleavage shown in eqn. (1) (Scheme 1),<sup>5</sup> while alkylphenoxide anions fragment by simple homolytic cleavage (eqn. (2)), or following rearrangement (eqn. (3)).<sup>6</sup> When there is no simple fragmentation that can occur through the substituent, specific retro-cleavage of the phenyl ring occurs (see eqn. (4)).<sup>7</sup>

The collision induced mass spectrum of deprotonated (methyl- $d_3$ ) benzoate is shown in Fig. 1. The spectrum is unusual in that the major fragmentation involves loss of carbon monoxide from the even-electron parent anion. This paper addresses the following questions: (i) does loss of CO from deprotonated methyl benzoate only occur when the deprotonation occurs at the *ortho* position, or does the process also occur for the isomeric anions formed by deprotonation at the *meta* and *para* positions on the phenyl ring? (ii) Is the loss of CO a charge-remote reaction, *i.e.* a fragmentation not directed by the negative charge on the ring? (iii) If the loss of CO process is not a charge-remote process, what is the mechanism?



Scheme 1

## Results and discussion

The reaction between (methyl- $d_3$ ) benzoate and  $HO^-$  in the ion source of the mass spectrometer produces only an  $(M - H)^-$  ion. Collisional activation of this anion results in loss of CO (Fig. 1). The only deprotonated esters that have been reported to lose CO are dimethyl succinate (where the loss is a minor process)<sup>8</sup> and acyloxy acetates (where the loss constitutes the base peak of the spectrum).<sup>9</sup> In both cases, an incipient  $MeOCO^-$  ion acts as a  $MeO^-$  donor within an anion–neutral–ion complex (the reaction  $MeOCO^- \rightarrow MeO^- + CO$  is exothermic by 2 kJ mol $^{-1}$ ).<sup>10</sup> The latter reaction occurs following the (acyloxy)acetate–acylhydroxyacetate rearrangement (eqn. (5), Scheme 2).<sup>9</sup> We have also, for comparison, measured the

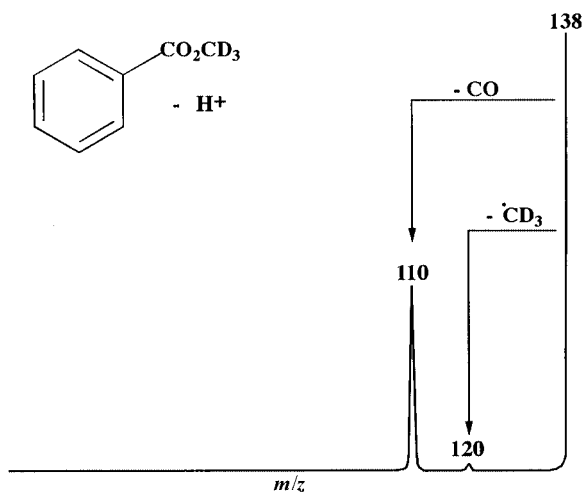
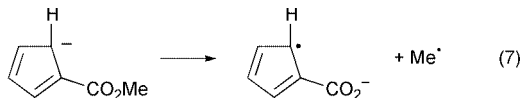
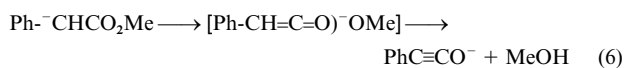
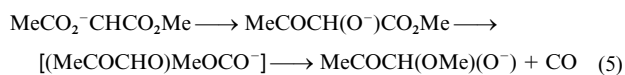


**Fig. 1** Collisional activation (CA) mass spectrum (MS/MS) of deprotonated (methyl- $d_3$ ) benzoate. VG ZAB 2HF mass spectrometer. For experimental conditions see Experimental section.

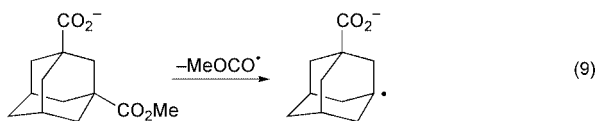
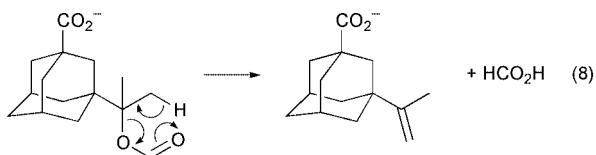
mass spectra of several deprotonated esters which contain unsaturation: these show simple fragmentation processes, for example, deprotonated methyl phenylacetate fragments as shown in eqn. (6), Scheme 2, while the major fragmentation of deprotonated cyclopentadienyl ester is loss of the ester substituent (eqn. (7), Scheme 2). Neither of these examples show



**Scheme 2**

loss of CO. It is also of interest to note that the fragmentation behaviour of deprotonated methyl benzoate (an even-electron anion) is quite different from that of radical anions (odd-electron anions) of the general formula  $\text{ArCO}_2\text{R}^-$ : these show the characteristic cleavage sequence  $\text{M}^{\cdot-} - \text{R}^{\cdot} - \text{CO}_2$ .<sup>11</sup>

There has been much debate recently concerning charge-remote reactions, *i.e.* reactions that occur remote from and uninfluenced by the charged centre.<sup>3,4</sup> Such reactions may occur when simple fragmentations are energetically unfavourable. We have studied charge-remote reactions using 1,3-disubstituted adamantanes, systems where the charged centre and the reacting centre are separated by a rigid saturated ring system, and cannot approach through space. A particular example of a charge-remote reaction is the facile loss of formic acid from the species shown in eqn. (8), Scheme 3.<sup>5</sup> Perhaps the loss of CO from deprotonated methyl benzoate is a charge-remote reac-



**Scheme 3**

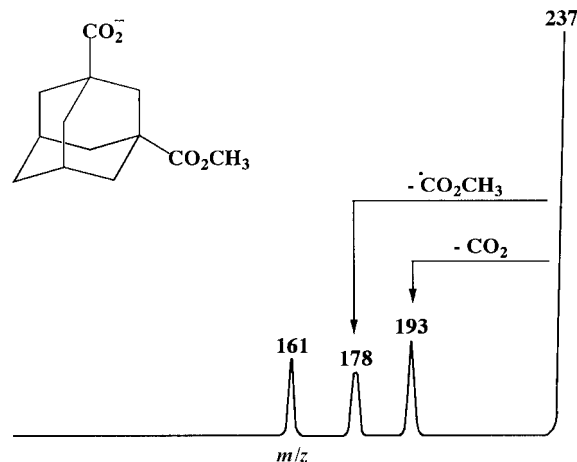


**Fig. 2** CA MS/MS of the carboxylate anion produced by the  $\text{S}_{\text{N}}2$  reaction between  $\text{HO}^-$  and 1,3-bis(methoxycarbonyl)adamantane in the ion source of the VG 2HF mass spectrometer. The peak at  $m/z$  161 in this spectrum is formed by the sequence  $[(\text{M} - \text{H})^- - (\text{CO}_2 + \text{MeOH})]$ .

tion? In order to test this proposal, we have measured the collision induced mass spectrum of the adamantane ester shown in Fig. 2. A charge-remote radical cleavage reaction occurs (eqn. (9), Scheme 3), but no loss of CO is noted. We conclude from all the above data that the loss of CO from deprotonated methyl benzoate is charge initiated and that the aryl ring system is a prerequisite for this reaction.

If the loss of CO from deprotonated (methyl- $d_3$ ) benzoate is charge initiated, is the reaction initiated by the charge being at the *ortho* position of the ring, or can it also occur for those isomers where the charges are localised on *meta* or *para* positions? Deprotonation of the phenyl ring of (methyl- $d_3$ ) benzoate with  $\text{HO}^-$ , can, in principle, occur at any ring position, so the spectrum shown in Fig. 1 does not answer this question. We have approached this problem both indirectly and directly. First, we examined the collision induced mass spectrum of an analogous compound which has *ortho* and *para* positions blocked so that deprotonation can only occur in the *meta* positions. The compound chosen was methyl 2,4,6-trifluorobenzoate: the spectrum of the  $(\text{M} - \text{H})^-$  ion shows the two major fragmentations  $[(\text{M} - \text{H})^- - \text{HF}]$  and  $[(\text{M} - \text{H})^- - \text{MeCO}_2]$  in the ratio of 2:1. Both of these fragmentations are high energy processes [even though the electron affinity of  $\text{F}^{\cdot}$  is 3.4 eV,<sup>12</sup> the C-F bond energy is high (543.9 kJ mol<sup>-1</sup>)<sup>13</sup>]. Since no loss of CO from this parent anion is observed, this might suggest that (methyl- $d_3$ ) benzoate deprotonated at the *meta* position should not fragment by loss of carbon monoxide. On the other hand it may be that in the trifluoro system, loss of CO is not observed because it is energetically unfavourable with respect to the competing reactions, *viz.* the loss of HF.

In order to confirm this proposal it is necessary to prepare the required three isomeric anions unequivocally and to obtain their mass spectra. We chose to use the  $\text{S}_{\text{N}}2(\text{Si})$  procedure (initially proposed by DePuy *et al.*<sup>14</sup>) for this purpose, *viz.*  $\text{RSiMe}_3 + \text{Nu}^- \rightarrow \text{R}^- + \text{Me}_3\text{SiNu}$ . The neutral precursors methyl (*ortho*-, *meta*- and *para*-trimethylsilyl)benzoate were synthesised and the collision induced mass spectra of the three isomeric anions are shown in Figs. 3-5. The mass spectrum of the *ortho* isomer (Fig. 3) is dominated by loss of CO, and is comparable with that shown in Fig. 1. This confirms that the *ortho* isomer undergoes pronounced loss of CO. The most surprising feature of these experiments is that the *meta* and *para* isomers also lose carbon monoxide. A qualitative estimate of the CO loss from each of the isomeric anions can be obtained by comparing the abundances of the peaks formed from  $[(\text{M} - \text{H})^- - \text{CO}]$  and  $[(\text{M} - \text{H})^- - \text{Me}^{\cdot}]$  processes in the three

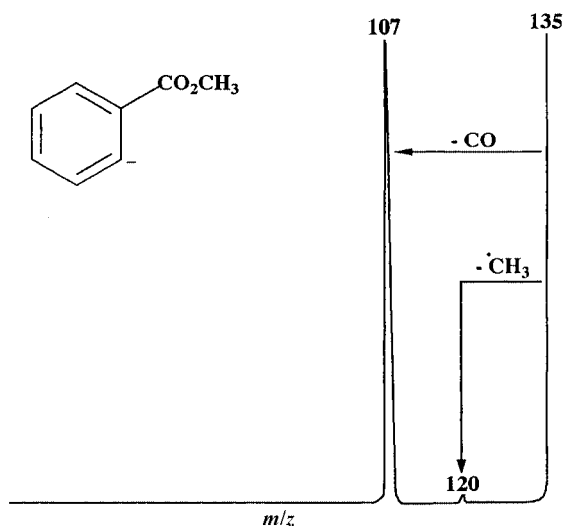


Fig. 3 CA MS/MS of the methyl *o*-benzoate anion formed by the  $S_N2(Si)$  reaction between  $HO^-$  and methyl *o*-trimethylsilylbenzoate.

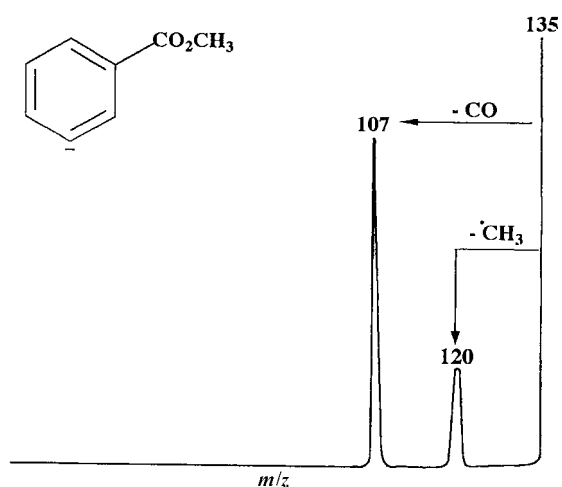


Fig. 4 CA MS/MS of the methyl *m*-benzoate anion formed by the  $S_N2(Si)$  reaction between  $HO^-$  and methyl *m*-trimethylsilylbenzoate. VG ZAB 2HF mass spectrometer.

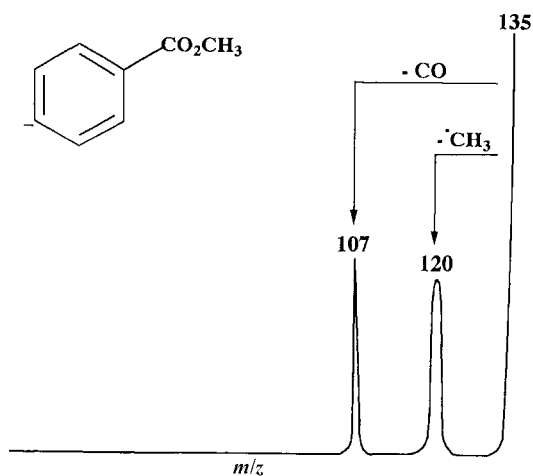


Fig. 5 CA MS/MS of the methyl *p*-benzoate anion formed by the  $S_N2(Si)$  reaction between  $HO^-$  and methyl *p*-trimethylsilylbenzoate. VG ZAB 2HF mass spectrometer.

spectra, viz. *ortho* (100:3), *meta* (100:28) and *para* (100:91). The energy required for loss of  $Me^\cdot$  is comparable in each case, so the relative extent of CO loss is *ortho*  $\gg$  *meta*  $>$  *para*. The peak widths at half height of the three *m/z* 107 ions in Figs. 2 to 4 are different [*ortho* (28.0 V), *meta* (32.9 V) and *para* (35.7 V)].

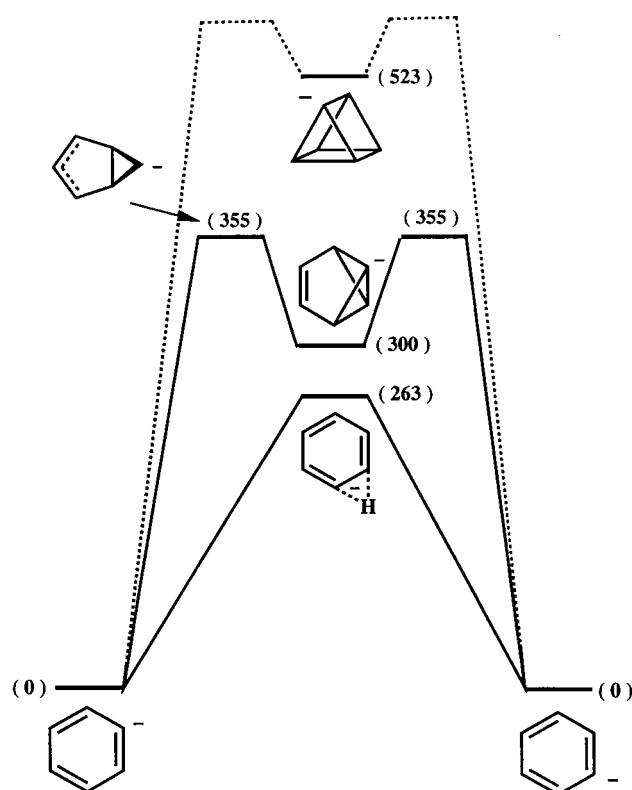


Fig. 6 Possible phenyl anion interconversions. B3LYP/6-311++G(d,p)//HF/6-31+G(d) level of theory. Full details of energies and geometries and species shown in the figure are listed in Table 1.

This means that either the structures and/or energies of the three *m/z* 107 ions are different, or their modes of formation are different.<sup>15</sup> The three *m/z* 107 ions are also formed in the ion source of the mass spectrometer. These three ions show the characteristic loss of  $CH_2O$  from the  $(M - H)^-$  ion of anisole.<sup>16,17</sup> Not only that, but the peak widths of the three *m/z* 77 ( $C_6H_5^-$ ) species formed by loss of  $CH_2O$  from the three source-formed *m/z* 107 ions are the same within experimental error ( $33.5 \pm 0.5$  V) and the same as the peak formed by loss of  $CH_2O$  from *ortho*- $(C_6H_4)OMe$  [formed by the  $S_N2(Si)$  reaction between  $HO^-$  and *ortho*-trimethylsilylanisole]. The experimental measurements indicate that the three product ions (*m/z* 107) formed by losses of CO from the *ortho*, *meta*, and *para* isomers of  $[(C_6H_4)CO_2Me]^-$  have the same structure [the *ortho* anion of  $(C_6H_4)OMe$ ], but the energetics of formation of this anion from each precursor are different. We propose from the available data, that the loss of carbon monoxide is a reaction of the *ortho* anion  $[(C_6H_4)CO_2Me]^-$ , and that the losses of CO observed in the spectra of *meta* and *para* isomers are a consequence of rearrangement of these isomers to the *ortho* anion prior to loss of CO.

Mechanisms which may account for the interconversion of the *ortho*, *meta* and *para* forms of deprotonated methyl benzoate are, (i) C scrambling via a prismane-type anion, (ii) C scrambling via stepwise formation and cleavage of benzvalene anions, (iii) a process by which H is transported around the phenyl ring leaving the carbon framework unchanged, or (iv) a combination of some of the above. Some data concerning the energetics of C scrambling in neutral benzene have been examined by theoretical and experimental studies indicating that these are energetically unfavourable processes.<sup>18-20</sup> The relative energies [at the RMP2/6-31G(d) level of theory] of benzvalene and prismane relative to benzene are 313 and 492  $kJ\ mol^{-1}$  respectively.<sup>18</sup> The energy of the transition state for ring opening of benzvalene is calculated to be 116  $kJ\ mol^{-1}$  above benzvalene (at the B3LYP/DZP level of theory)<sup>19,20</sup> and measured experimentally to be 122.6  $kJ\ mol^{-1}$ .<sup>21</sup>

**Table 1** Geometries (bond lengths/Å, angles/° and dihedral angles/°) and energies for species in Fig. 6 (geometries—HF/6-31+G(d), energies—B3LYP/6-311++G(d,p))

	1	2	3
Energy/hartree	-231.6593903	-231.5529727	-231.5431464
Zero pt correction	0.091767	0.084772	0.089399
Relative Energy/ kJ mol <sup>-1</sup>	0.0	262.6	299.5

	4	5
Energy/hartree	-231.5163550	-231.4574589
Zero pt correction	0.085732	0.088729
Relative Energy/ kJ mol <sup>-1</sup>	355.4	522.9

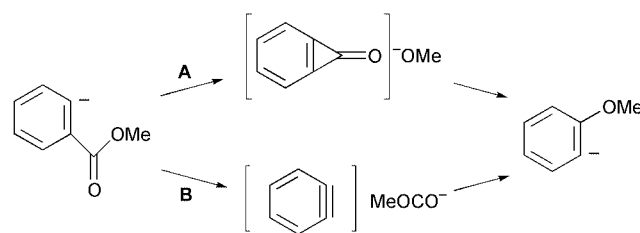
	1	2	3	4	5
C2–C1	1.417	1.435	1.580	1.504	1.545
C3–C2	1.394	1.394	1.500	1.455	1.546
C4–C3	1.391	1.397	1.332	1.386	1.503
C5–C4	1.391	1.391	1.501	1.383	1.507
C6–C5	1.394	1.397	1.495	1.502	1.546
H7–C2	1.084	1.288	1.080	1.083	1.082
H8–C3	1.082	1.082	1.077	1.074	1.081
H9–C4	1.080	1.081	1.077	1.079	1.082
H10–C5	1.082	1.081	1.080	1.076	1.081
H11–C6	1.084	1.082	1.086	1.093	1.082
C3–C2–C1	124.8	119.4	111.3	129.6	92.7
C4–C3–C2	120.3	120.2	105.1	107.5	89.1
C5–C4–C3	117.9	120.4	105.1	111.7	60.8
C6–C5–C4	120.3	120.4	109.6	113.1	89.1
H7–C2–C1	118.7	56.1			129.7
H7–C2–C3				121.5	118.7
H8–C3–C2	120.1	121.1	126.4	124.0	133.8
H9–C4–C3	121.0	120.1	128.4	125.4	127.8
H10–C5–C4	119.5	119.5	121.5	125.7	130.4
H11–C6–C5	116.4	118.7	135.3	119.6	130.2
C4–C3–C2–C1			31.8	40.7	-1.2
C5–C4–C3–C2			0.0	8.3	-90.2
C6–C5–C4–C3			-29.1	4.5	59.6
H7–C2–C3–C4			179.5	-166.1	-152.5
H8–C3–C4–C5			178.8	155.6	116.2
H9–C4–C3–H8			0.0	-171.0	-0.8
H10–C5–C4–H9			-0.7	-176.7	0.8
H11–C6–C5–H10			-24.0	139.2	0.5

We have calculated the reaction coordinates for the interconversion of the phenyl and benzvalene anions at the modest B3LYP/6-311++G(d,p)//HF/6-31+G(d) level of theory and the results are summarised in Fig. 6 and Table 1. At this level of theory, the benzvalene anion lies 300 kJ mol<sup>-1</sup> above the phenyl anion, and the transition state for interconversion of the two is 355 kJ mol<sup>-1</sup> above the phenyl anion. The corresponding prismane anion is 523 kJ mol<sup>-1</sup> less stable than the phenyl anion. The formation of this anion is clearly not feasible in comparison to formation of the benzvalene anion, thus we have not calculated the transition state for this interconversion.

Anion scrambling *via* a degenerate H transfer mechanism is also shown in Fig. 6. The transition state is 263 kJ mol<sup>-1</sup> above the phenyl anion at the B3LYP/6-311++G(d,p)//HF/6-31+G(d) level of theory, making this a more energetically favoured process than that involving C scrambling through a

benzvalene anion. We have also computed the transition state energies for the equivalent H migration reactions of deprotonated methyl benzoate at the same level of theory, and these reactions are summarised in Fig. 7. It appears that there is no significant difference in the energetics of the H transfer process for the phenyl anion and deprotonated methyl benzoate. On the basis of these calculations, we propose that the interconversions of *ortho*, *meta* and *para* anions occur by H transfers. The interconversions *meta* to *ortho*, and *para* to *ortho* require one and two steps respectively, explaining the observed CO loss ratio *meta* > *para*.†

There are two possible mechanisms which could account for the loss of CO from deprotonated methyl benzoate. The first, route A (Scheme 4), involves a cyclisation and nucleophilic



**Scheme 4**

substitution prior to loss of CO. The second involves the formation of a [benzynes–MeOCO<sup>-</sup>] ion complex, followed by a cine substitution with MeOCO<sup>-</sup> acting as a MeO<sup>-</sup> donor. We have investigated the reaction coordinates of both of these reaction pathways using calculations at the B3LYP/6-311++G(d,p)//HF/6-31G+(d) level of theory. The two mechanistic pathways are shown in Figs. 8 and 9; structures and energies of the reactant, transition states, reactive intermediates and products are shown in Table 2.

The cyclisation process A shown in Fig. 8 has four steps, with the initial cyclisation step together with the subsequent attack of the incipient MeO<sup>-</sup> at a ring carbon being rate determining with a barrier of 202 kJ mol<sup>-1</sup> at this level of theory. The benzyne cine substitution mechanism B is shown in Fig. 9. This is a simpler process than that shown in Fig. 8, but the barrier to the transition state for the benzyne mechanism is 289 kJ mol<sup>-1</sup>, some 87 kJ mol<sup>-1</sup> more than that for cyclisation process A. Thus the cyclisation process is favoured in terms of the relative barriers to the respective transition states of the rate determining steps. There is however, a second factor which must be taken into account when determining the relative rates of these two processes, *viz.* the relative pre-exponential Arrhenius factors for both processes. In other words, there may be entropy bottlenecks in such reactions. In principle, the larger the number of steps, the greater the probability of such bottlenecks. In order to access these factors properly, we need to know the potential surfaces for both processes, *i.e.* the width of the pathways of each step into and out of each transition state and reactive intermediate, together with the curvature of the reaction coordinate pathway. Unfortunately, such calculations are not feasible with a system of this size using our supercomputing facilities. What we can do however, is to compare the relative vibrational partition functions of the first transition state in each of the two mechanisms: this will give some insight into the relative values of the pre-exponential factors for each of the processes A and B. We have described this method (together

† A reviewer has suggested that the anion interconversion could be due to H exchange within an anion–water complex, *viz.* [(*m*-C<sub>6</sub>H<sub>4</sub>CO<sub>2</sub>Me)<sup>-</sup>(H<sub>2</sub>O)] → [(*o*-C<sub>6</sub>H<sub>4</sub>CO<sub>2</sub>Me)(HO<sup>-</sup>)] → [(*o*-C<sub>6</sub>H<sub>4</sub>CO<sub>2</sub>Me)<sup>-</sup>(H<sub>2</sub>O)] → [(*o*-C<sub>6</sub>H<sub>4</sub>CO<sub>2</sub>Me)<sup>-</sup> + H<sub>2</sub>O]. We have tested this proposal by allowing the *o*, *m* and *p* anions formed by the respective S<sub>N</sub>2(Si) reactions to be exposed to D<sub>2</sub>O in the ion source. No incorporation of D into the anions is observed, thus this process is not operable.

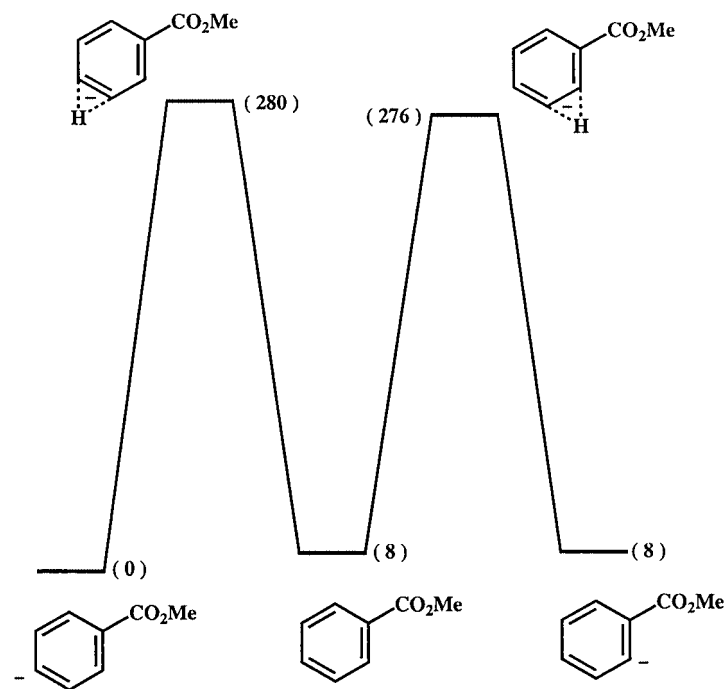


Fig. 7 H transfer reactions within deprotonated methyl benzoate. B3LYP/6-311++G(d,p)//HF/6-31+G(d) level of theory.

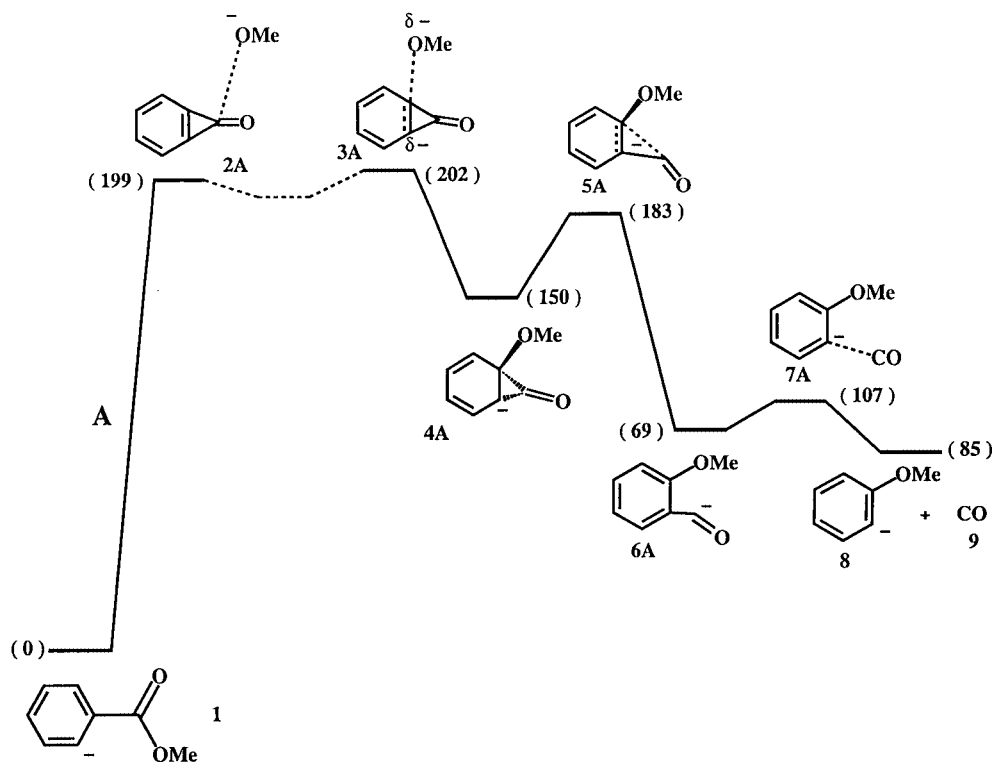


Fig. 8 Loss of CO from the methyl *o*-benzoate anion. The cyclisation mechanism A. B3LYP/6-311++G(d,p)//HF/6-31+G(d) level of theory. Full details of energies and geometries of reactant, reactive intermediates, transition states and products are listed in Table 2.

with its approximations) in detail previously<sup>22</sup> (see also ref. 23). These data are recorded in Table 3.

There is a difficulty in knowing precisely which of the low frequency vibrations (shown in Table 3) to use, but if all of the listed values are considered, the Arrhenius factor for the benzyne process **B** is some four times larger than that for process **A**. This is clearly a maximum value, but it is in the correct direction, since the first transition state for dissociative process **A** has a number of low frequency modes for which there are no counterparts in the first transition state for **B**.

In conclusion, the loss of carbon monoxide from deproton-

ated methyl benzoate to form deprotonated anisole, is initiated from an anion in which the charge is localised on the *ortho* position of the phenyl ring. If the initial anion centre is situated *meta* or *para* to the methoxycarbonyl substituent, 1,2-H transfer(s) effects formation of the *ortho* anion prior to fragmentation of the substituent. We are not able, using the available data, to differentiate between the two mechanisms shown in Scheme 4. The barrier to the first transition state for the cyclisation process **A** is 87 kJ mol<sup>-1</sup> lower than that for benzyne mechanism **B** at the level of theory used, but this is counteracted by the Arrhenius factor for the process **A** being the smaller of the two.

**Table 2** Geometries and energies of all species in Figs. 8 and 9 (geometries—HF/6-31+G(d), energies—B3LYP/6-311++G(d,p))

A Reactants and products						
Energy/hartree	-459.6162298	-346.2297129	-113.3485635			
Zero pt correction	0.138628	0.126984	0.005542			
Relative Energy of Reactant/kJ mol <sup>-1</sup>	0.0					
Relative Energy of Product/kJ mol <sup>-1</sup>		85.0				
	<b>1</b>	<b>8</b>	<b>9</b>			
O2-C1			1.113			
C2-C1	1.425	1.409				
C3-C2	1.413	1.399				
C4-C3	1.408	1.393				
C5-C4	1.377	1.389				
C6-C5	1.401	1.389				
C7-C3	1.487					
O7-C3		1.388				
O8-C7	1.209					
C8-O7		1.390				
O9-C7	1.332					
C10-O9	1.399					
C3-C2-C1	112.2	112.0				
C4-C3-C2	124.4	125.4				
C5-C4-C3	120.3	119.5				
C6-C5-C4	118.2	119.3				
C7-C3-C2	121.3					
O7-C3-C2		121.8				
O8-C7-C4	125.0					
C8-O7-C3		118.3				
O9-C7-C8	119.7					
C10-O9-C7	117.1					
<b>B Other species in Fig. 8</b>						
Energy/hartree	-459.5353556	-459.5348882	-459.5577180	-459.5421810	-459.5883092	-459.5719478
Zero pt correction	0.133144	0.13364	0.137261	0.134011	0.136638	0.134734
Relative Energy/kJ mol <sup>-1</sup>	199.2	201.6	150.3	183.3	68.5	106.9
	<b>2A</b>	<b>3A</b>	<b>4A</b>	<b>5A</b>	<b>6A</b>	<b>7A</b>
C2-C1	1.395	1.426	1.442	1.477	1.396	1.481
C3-C2	1.352	1.370	1.496	1.511	1.397	1.474
C4-C3	1.395	1.435	1.493	1.424	1.394	1.346
C5-C3	1.378	1.351	1.341	1.370	1.385	1.436
C6-C5	1.420	1.454	1.466	1.458	1.389	1.397
C7-C2	1.440	1.389	1.355	1.296	1.614	1.313
C8-C7	1.194	1.207	1.222	1.181	1.223	1.181
O9-C3	2.666	2.102	1.422	1.412	1.370	1.380
C10-O9	1.346	1.348	1.389	1.391	1.406	1.383
C3-C2-C1	123.6	123.8	123.8	120.3	116.5	114.9
C4-C3-C2	123.6	121.2	113.3	112.4	121.4	121.8
C5-C4-C3	114.0	114.6	119.2	121.9	120.5	122.6
C6-C5-C4	122.4	123.1	121.9	119.9	119.3	116.6
C7-C2-C3	62.0	62.1	62.5	86.4	123.4	121.2
O8-C7-C2	147.8	151.0	151.9	173.3	110.0	177.2
O9-C3-C2	75.3	118.7	121.6	120.5	123.1	111.9
C10-O9-C3	144.4	116.6	114.7	115.2	116.7	118.8
C4-C3-C2-C1	0.0	-11.7	-21.4	-30.6	-0.9	0.0
C5-C4-C3-C2	-2.1	8.7	17.8	8.2	0.9	0.0
C6-C5-C4-C3	2.1	-1.0	-3.8	14.5	-0.2	0.0
C7-C2-C3-C4	-175.6	148.9	113.2	114.0	-179.4	180.0
O8-C7-C2-C3	-147.5	-172.2	-171.1	-171.2	-162.8	180.0
O9-C3-C2-C1	115.2	99.0	117.3	113.3	-178.0	180.0
C10-O9-C3-C2	111.5	27.7	-58.0	-64.8	-67.6	180.0

Table 2 (continued)

C Other species in Fig. 9

	2B	3B	4B
Energy/hartree	-459.5034321	-459.5052152	-459.4998809
Zero pt correction	0.132472	0.131411	0.131642
Relative Energy/ kJ mol <sup>-1</sup>	281.4	274.2	288.7

	2B	3B	4B
C2-C1	1.417	1.408	1.418
C3-C2	1.251	1.366	1.250
C4-C3	1.360	1.400	1.359
C5-C4	1.398	1.408	1.397
C6-C5	1.405	1.394	1.409
C7-C4		3.581	3.320
O8-C7	1.221	1.203	1.204
O9-C7	1.416	1.492	1.480
C10-O9	1.397	1.391	1.392
C3-C2-C1	110.1	114.0	109.6
C4-C3-C2	105.6	140.0	143.4
C5-C4-C3	121.3	105.5	105.7
C6-C5-C4	121.9	121.9	121.2
C7-C3-C2	146.0		
C7-C4-C3		169.1	96.8
O8-C7-C4		174.9	175.1
O8-C7-C3	98.4		
O9-C7-C8	113.1	11.9	112.3
C10-O9-C7	118.7	118.4	118.5

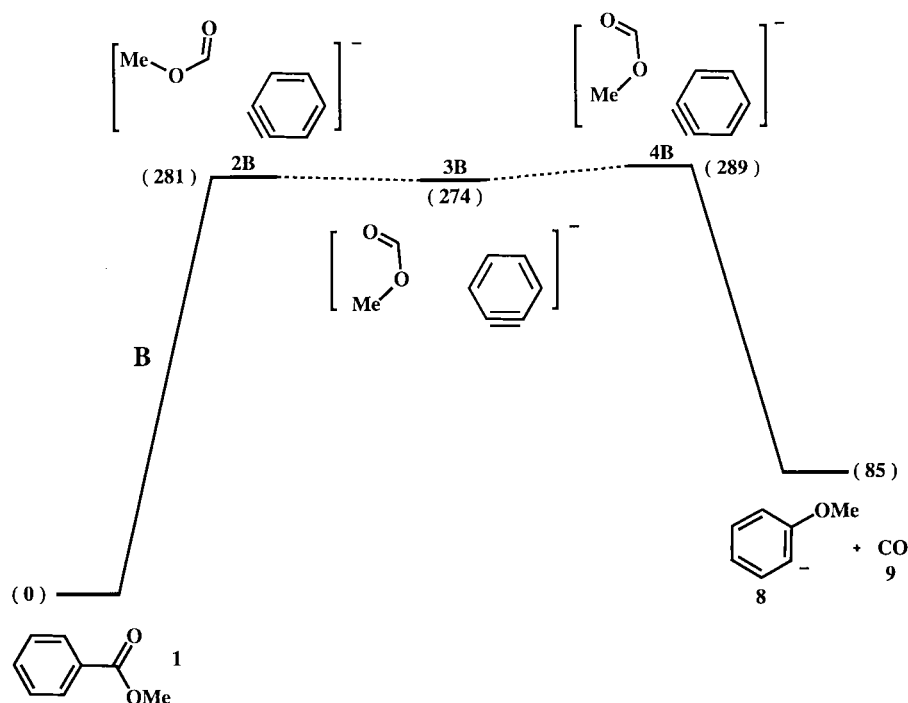


Fig. 9 Loss of CO from the methyl *o*-benzoate anion. The benzyne mechanism B. B3LYP/6-311G(d,p)//HF/6-31+G(d) level of theory. Details of energies and geometries of species shown in the figure are listed in Table 2.

## Experimental

### A. Synthetic procedures

Methyl benzoate and methyl phenylpropiolate were commercial samples used without further purification. The following compounds were made by reported procedures: 1-methoxycarbonylcyclopenta-1,3-diene,<sup>24</sup> methyl *o*-trimethylsilylbenzoate,<sup>25</sup>

methyl *m*-trimethylsilylbenzoate,<sup>26</sup> methyl *p*-trimethylsilylbenzoate,<sup>27</sup> and *o*-trimethylsilylanisole.<sup>28</sup> (Methyl-*d*<sub>3</sub>) benzoate (*d*<sub>3</sub> = 99%) was prepared by esterification of benzoyl chloride with methanol-*d*<sub>4</sub>.<sup>29</sup>

### B. Computational methods

Geometry optimisations were carried out at the HF/6-31+G(d)

**Table 3** Vibrational partition functions ( $Q'$  vib) for transition states **2A** and **2B**

Transition state <b>2A</b>		Transition state <b>2B</b>	
Frequency/cm <sup>-1</sup>	$Q'$ vib	Frequency/cm <sup>-1</sup>	$Q'$ vib
63	4.1394	38	6.5088
92	3.0050	59	4.3730
100	2.8028	99	2.8205
112	2.5641	105	2.6986
183	1.8067	134	2.2487
269	1.4412	185	1.7914
293	1.3802	342	1.2851
394	1.2144	361	1.2553
499	1.1251	443	1.1657
548	1.0984	466	1.1473
584	1.0827	480	1.1373
688	1.0507	666	1.0560
771	1.0347	691	1.0501
807	1.0295	759	1.0366
823	1.0274	845	1.0248
843	1.0250	902	1.0192
972	1.0140	926	1.0172
1063	1.0094	966	1.0144
1079	1.0087	1074	1.0089
1103	1.0078	1075	1.0088
1113	1.0075	1096	1.0081
1181	1.0055	1122	1.0072
1242	1.0042	1158	1.0061
1244	1.0042	1204	1.0050
1247	1.0041	1227	1.0045
1282	1.0035	1274	1.0037
1289	1.0034	1309	1.0031
1399	1.0021	1340	1.0027
1401	1.0021	1411	1.0020
1584	1.0009	1530	1.0012
1607	1.0008	1594	1.0009
1609	1.0008	1596	1.0009
1626	1.0008	1630	1.0008
1626	1.0008	1644	1.0007
1770	1.0004	1649	1.0007
1785	1.0004	1724	1.0005
1980	1.0002	1997	1.0002
2870	1.0000	3178	1.0000
2907	1.0000	3225	1.0000
2976	1.0000	3230	1.0000
3325	1.0000	3321	1.0000
3345	1.0000	3343	1.0000
3375	1.0000	3362	1.0000
3378	1.0000	3374	1.0000

level of GAUSSIAN 94.<sup>30</sup> Energies were optimised by the Becke 3LYP method<sup>31,32</sup> *i.e.* B3LYP/6-311++G(d,p)//HF/6-31+G(d). The calculated frequencies were also used to determine the zero-point vibrational energies which were then scaled by 0.9135<sup>33</sup> and used as a zero-point energy correction for the electronic energies calculated at this and higher levels of theory. Stationary points were characterised as either minima (no imaginary frequencies) or transition states (one imaginary frequency) by calculation of the frequencies using analytical gradient procedures. The minima connected by a given transition structure were confirmed by intrinsic reaction coordinate (IRC) calculations. Calculations were carried out using the Power Challenge Super Computers at the South Australian Super Computing Centre (The University of Adelaide), and the Beowulf computing cluster at the South Australian Computational Chemistry Facility (The University of Adelaide).

### C. Mass spectrometric methods

Collisional activation mass spectra (CA MS/MS) were measured using a two-sector reversed geometry VG ZAB 2HF spectrometer. This instrument and the typical experimental conditions of negative ion chemical ionisation (NICI) have

been described in detail elsewhere.<sup>34</sup> Samples were introduced into the source *via* a heated septum inlet, producing a measured pressure of  $5 \times 10^{-6}$  Torr inside the source housing. Typical ionization conditions were: source temperature, 200 °C; ionising energy, 70 eV (tungsten filament); accelerating voltage, -7 kV. All slits were fully open in order to minimize mass discrimination effects due to energy resolution.<sup>35,36</sup> The reagent ion HO<sup>-</sup> was generated from electron impact on H<sub>2</sub>O (introduced through the heated septum inlet to give an operating pressure inside the source housing of *ca.*  $5 \times 10^{-5}$  Torr, and thus an estimated pressure inside the ion source of close to 0.1 Torr). Negative ion chemical ionisation of the sample either effected (i) deprotonation, or (ii) desilylation of a neutral trimethylsilylated substrate, by analogy to the method originally developed by DePuy *et al.*<sup>14</sup> Collisional activation (CA) spectra were obtained by collision of the incident anions with argon in the first of two collision cells at a pressure typically around  $10^{-7}$  Torr. This reduces the main beam to 90% of its initial value, producing essentially single collision conditions in the collision cell.<sup>37</sup> Peak width (at half height) values are a mean of ten measurements and are correct to within  $\pm 0.5$  V.

### Acknowledgements

We thank the Australian Research Council for funding this work. S. D. thanks the ARC for a research associate stipend. We thank Mark S. Taylor (University of Colorado, Boulder) for helpful discussion concerning the calculation of vibrational partition functions.

### References

- 1 J. H. Bowie, The Fragmentations of (M - H)<sup>-</sup> Ions Derived from Organic Compounds: an Aid to Structure Determination, in *Topics in Mass Spectrometry. Vol. 1. Experimental Mass Spectrometry*, ed. D. H. Russell, pp. 1-34, Plenum Press, New York and London, 1994.
- 2 S. Dua, P. C. H. Eichinger, G. W. Adams and J. H. Bowie, *Int. J. Mass Spectrom. Ion Processes*, 1994, **133**, 1.
- 3 J. Adams, *Mass Spectrom. Rev.*, 1990, **9**, 141; M. L. Gross, *Int. J. Mass Spectrom. Ion Processes*, 1992, **118/119**, 137.
- 4 S. Dua, J. H. Bowie, B. A. Cerda and C. Wesdemiotis, *J. Chem. Soc., Perkin Trans. 2*, 1998, 1443.
- 5 M. J. Raftery, J. H. Bowie and J. C. Sheldon, *J. Chem. Soc., Perkin Trans. 2*, 1988, 563.
- 6 L. B. Reeks, P. C. H. Eichinger and J. H. Bowie, *Rapid Commun. Mass Spectrom.*, 1993, **7**, 286.
- 7 J. H. Bowie, *Mass Spectrom. Rev.*, 1990, **9**, 349, and references cited therein.
- 8 M. J. Raftery and J. H. Bowie, *Aust. J. Chem.*, 1987, **47**, 711.
- 9 P. C. H. Eichinger, R. N. Hayes and J. H. Bowie, *J. Am. Chem. Soc.*, 1991, **113**, 1949.
- 10 Thermochemical data from <http://webbook.nist.gov>
- 11 A. C. Ho, J. H. Bowie and A. Fry, *J. Chem. Soc. B*, 1971, 530.
- 12 P. L. Jones and R. D. Mead, *J. Chem. Phys.*, 1980, **73**, 4419.
- 13 S. W. Benson, *Thermochemical Kinetics*, Wiley, New York, 1968.
- 14 C. H. DePuy, V. M. Bierbaum, L. A. Flippin, J. J. Grabowski, G. K. King, R. J. Schmitt and S. A. Sullivan, *J. Am. Chem. Soc.*, 1980, **102**, 5012.
- 15 For discussions of metastable and collision induced ions see, R. G. Cooks, J. H. Beynon, R. M. Caprioli and G. R. Lester, *Metastable Ions*, Elsevier, Amsterdam, London and New York, 1973.
- 16 T. C. Kleingeld and N. M. M. Nibbering, *Tetrahedron*, 1983, **39**, 4193.
- 17 P. C. H. Eichinger, J. H. Bowie and R. N. Hayes, *Aust. J. Chem.*, 1989, **42**, 865.
- 18 J. M. Schulman and R. L. Disch, *J. Am. Chem. Soc.*, 1985, **107**, 5059.
- 19 K. E. Wilzbach, J. S. Ritcher and J. L. Kaplan, *J. Am. Chem. Soc.*, 1971, **93**, 3782; M. J. S. Dewar and S. J. Krischner, *J. Am. Chem. Soc.*, 1975, **97**, 2932.
- 20 H. F. Bettinger, P. R. Schriener, H. F. Schaefer and P. von R. Schleyer, *J. Am. Chem. Soc.*, 1998, **120**, 5741.
- 21 N. J. Turro, C. A. Renner, T. J. Katz, K. B. Wiberg and H. A. Cannon, *Tetrahedron Lett.*, 1976, 4133.
- 22 J. M. Hevko, S. Dua, J. H. Bowie and M. S. Taylor, *J. Chem. Soc., Perkin Trans. 2*, 1999, 457.



- 23 R. G. Gilbert and S. C. Smith, *Theory of Unimolecular and Recombination Reactions*, Blackwell Scientific, Cambridge, UK, 1990; A. P. Scott and L. Radom, *J. Phys. Chem.*, 1996, **100**, 16502.
- 24 G. N. Grunewald and D. P. Davis, *J. Org. Chem.*, 1978, **43**, 3075.
- 25 A. G. Schultz and E. G. Antoulinakis, *J. Org. Chem.*, 1996, **61**, 4555.
- 26 C. Earborn and P. M. Jackson, *J. Chem. Soc. B*, 1969, 21.
- 27 J. C. Amedio, G. T. Lee, K. Prasad and O. Repic, *Synth. Commun.*, 1995, **25**, 2599.
- 28 D. S. Wilbur, W. E. Stone and W. S. Aderson, *J. Org. Chem.*, 1983, **48**, 1544.
- 29 R. A. McClelland and G. Patel, *J. Am. Chem. Soc.*, 1981, **103**, 6912.
- 30 GAUSSIAN 94, Revision C3, M. J. Frisch, G. W. Trucks, H. B. Schlegel, P. M. W. Gill, B. G. Johnson, M. A. Robb, J. R. Cheeseman, T. Keith, G. A. Petersson, J. A. Montgomery, J. B. Foresman, J. Cioslowski, B. B. Stefanov, A. Nanayakkara, M. Challacombe, C. Y. Peng, P. V. Ayala, W. Chen, M. W. Wong, J. L. Andres, E. S. Replogle, R. Gomperts, R. L. Martin, D. J. Fox, J. S. Binkley, D. J. Defrees, J. Baker, J. P. Stewart, M. Head-Gordon, C. Gonzales and J. A. Pople, Gaussian Inc., Pittsburgh, PA, 1995.
- 31 A. D. Becke, *J. Chem. Phys.*, 1993, **98**, 5648.
- 32 P. J. Stevens, F. J. Devlin, C. F. Chabrowski and M. J. Frisch, *J. Phys. Chem.* 1994, **98**, 11623.
- 33 M. W. Wong, *Chem. Phys. Lett.*, 1996, **256**, 391.
- 34 M. B. Stringer, J. H. Bowie and J. L. Holmes, *J. Am. Chem. Soc.*, 1986, **108**, 3888.
- 35 J. K. Terlouw, P. C. Burgers and J. L. Holmes, *Org. Mass Spectrom.*, 1979, **14**, 307.
- 36 P. C. Burgers, J. L. Holmes, A. A. Mommers and J. E. Szulejko, *J. Am. Chem. Soc.*, 1984, **106**, 521.
- 37 J. L. Holmes, *Org. Mass Spectrom.*, 1985, **20**, 169.